Creation and uses of positron plasmas*

R. G. Greaves,† M. D. Tinkle, and C. M. Surko
Physics Department, University of California, San Diego, La Jolla, California 92093-0319

(Received 4 November 1993; accepted 14 January 1994)

Advances in positron trapping techniques have led to room-temperature plasmas of 10^7 positrons with lifetimes of 10^3 s. Improvements in plasma manipulation and diagnostic methods make possible a variety of new experiments, including studies just being initiated of electron–positron plasmas. The large numbers of confined positrons have also opened up a new area of positron annihilation research, in which the annihilation cross sections for positrons with a variety of molecules have been measured, as well as the energy spread of the resulting gamma rays. Such measurements are of interest for fundamental physics and for the modeling of astrophysical plasmas.

I. INTRODUCTION

Positrons are the most easily obtainable form of antimatter in the laboratory, but until recently they have been studied only in single-particle interactions. Recent progress in the development of methods for trapping and storing positrons[1] now permits the accumulation of a sufficient number of low-temperature positrons to form a plasma.

Positrons are of interest to plasma physics because they annihilate electrons and because, having the same mass and opposite charge, positrons and electrons can be combined to form neutral plasmas with a dynamical symmetry between the charge species. Discussions of positrons in plasmas have ranged from the slowing down and annihilation of fast positrons in hydrogen plasmas[2–4] to the role that electron–positron plasmas might play in astrophysical situations.[5] The theory of the waves and instabilities expected in these plasmas predicts a variety of interesting phenomena unique to particle–antiparticle plasmas.[6,7]

The accumulation of large numbers of low-energy positrons now makes possible the experimental study of such unique systems, and of the related case of an electron beam traversing a positron plasma.[6] For electron–positron plasmas, both charge species are highly magnetized and one can go from a non-neutral to a neutral plasma by varying the relative density of electrons and positrons. Thus it will be possible to test new theories regarding the confinement of highly magnetized plasmas.

In addition to the motivation of studying plasma physics with positrons, the further development of methods to accumulate antimatter is likely to be crucial to the study of antimatter. At present, the only practical scheme for accumulation of low-energy antimatter is in the form of a non-neutral plasma.[8,9] The availability of large numbers of cold positrons allows us to study, under nearly ideal conditions, a number of other important physical phenomena involving the interaction of positrons with ordinary matter. Examples include the study of positron–molecule and positron–atom interactions below the threshold for positronium formation. These phenomena are directly relevant to gamma-ray astronomy.[10,11] The techniques developed here will also enable the accumulation of positrons for the production of antihydrogen.[12]

This paper is organized in the following way. In the next section, we briefly review the operation of our three-stage positron trap. In Secs. III and IV, we discuss techniques to diagnose and manipulate plasma parameters. Section V deals with the physics issues relating to electron–positron plasmas, while the techniques that have been proposed for creating such plasmas are discussed in Sec. VI. Section VII deals with the use of positron plasmas to study a variety of positron annihilation phenomena. In Sec. VIII, we discuss future improvements that are being considered, and Sec. IX concludes the paper.

II. THE POSITRON TRAP

The experimental apparatus used in this work consists of a radioactive source of positrons, a single-crystal tungsten transmission moderator, and a multistage positron trap, with associated magnetic-field coils and vacuum system.

The source of slow positrons is a radioactive ^{22}Na ($\tau_{1/2}=2.6$ yr) positron emitter used in conjunction with a tungsten moderator. This isotope emits positrons with energies up to 545 keV. The positrons impinge upon a single-crystal tungsten foil where a certain fraction of them are slowed to about 2 eV.[13,14] The positrons are magnetically guided from the moderator to the trapping region. The total efficiency of the combination of source and moderator is 2×10^{-4}.

The first three stages of the trap, which is shown schematically in Fig. 1, are formed by a set of eight cylindrically symmetrical electrodes. These electrodes form regions of decreasing electric potential, and they are constructed to allow three-stage differential pumping of the system, leading to three distinct regions of gas pressure. The high-pressure region (stage I) has a typical pressure of 10^{-3} Torr. The pressure in the middle region (stage II) is typically of the order of 10^{-4} Torr. Stage III forms the trapping region where the positrons are accumulated, and is operated at approximately 1×10^{-6} Torr. The electrode geometry of the third stage shown in Fig. 1 was based on

*Paper 3I6, Bull. Am. Phys. Soc. **38**, 1933 (1993).
†Invited speaker.

 1070-664X/94/1(5)/1439/8/$6.00

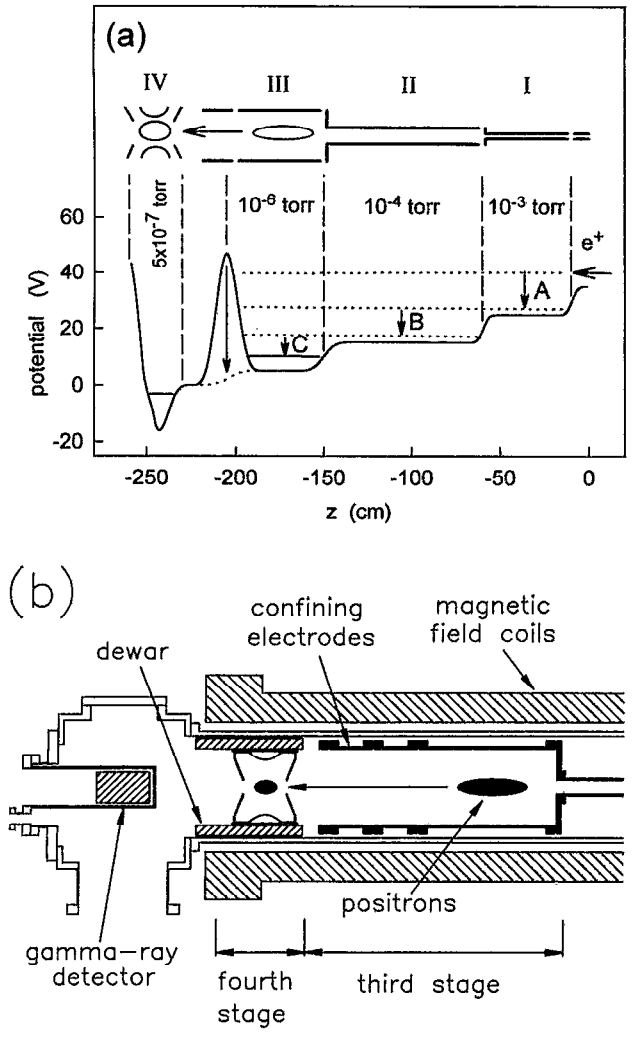

FIG. 1. (a) Four-stage electrode structure and axial electric potential profile of the positron trap. (b) Third and fourth stages of the trap showing the location of the hyperboloidal electrode assembly inside the liquid nitrogen dewar.

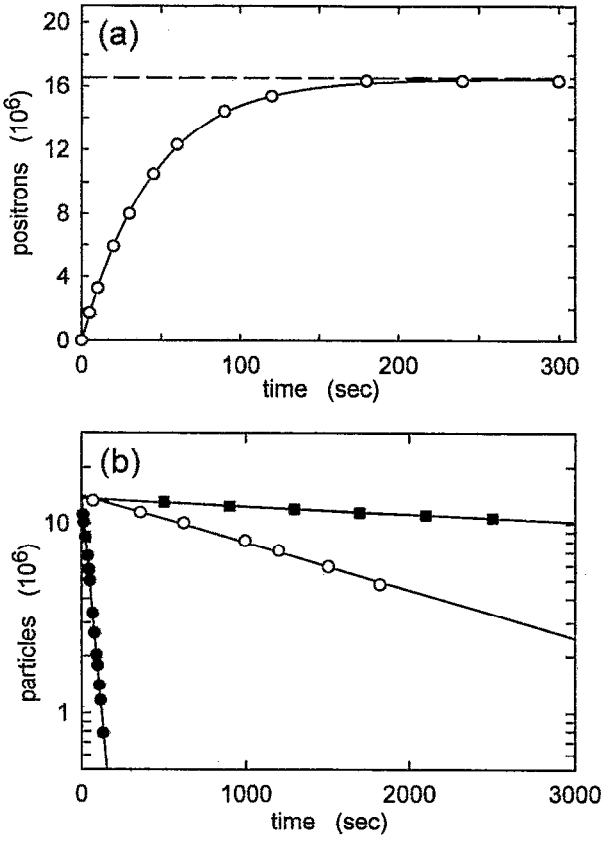

FIG. 2. (a) Accumulation of positrons. (b) Storage of positrons in the presence of a buffer gas at a pressure of 6×10^{-7} Torr (●). The fitted exponential yields a lifetime, $\tau=48$ s. Storage of particles with buffer gas feed switched off after loading particles ($P\simeq7\times10^{-10}$ Torr): positrons (○), and electrons (■). The fitted exponentials yield lifetimes of 0.5 and 2.8 h for positrons and electrons, respectively.

the highly successful experiments by Malmberg, Driscoll, and collaborators to confine pure-electron plasmas.[15,16] A magnetic field is applied along the axis of the trap using solenoids and is typically operated at approximately 1400 G.

Positrons enter the trap through stage I and accumulate in stage III by a series of inelastic collisions [designated "A", "B" and "C" in Fig. 1(a)]. The positrons trapped in region III cool to room temperature in a few seconds and form a plasma, which can be diagnosed and manipulated as described below.

Recently, we have added a fourth stage consisting of an electrode assembly with approximately hyperboloidal electrodes, as shown in Fig. 1(b). This new stage has served three functions. First, it has enabled us to study the low-order modes of spheroidal plasmas. Second, it has allowed us to demonstrate the stacking of positrons from the third to the fourth stage. Third, by moving the positron cloud closer to the gamma-ray detector shown in Fig. 1(b), it has improved the measurement of gamma-ray annihilation spectra from *in situ* annihilation of positrons.

During the past few years, we have systematically studied the physics of the trap operation and its optimization. The most recent improvement involved reconditioning the moderator by heat treatment in a low-pressure oxygen atmosphere. This reduced the energy spread of the emitted positrons, allowing the voltage difference between the moderator and first stage to be reduced from its previous optimum of about 15 V to about 9 V, which in turn reduced losses from positronium formation. This increased the trapping efficiency to 40%, i.e., to about twice its previous value. Further details of the operation of the trap and the trapping mechanism are given in Ref. 1.

As shown in Fig. 2(a), we are able to accumulate up to 1.6×10^7 positrons. The lifetime of positrons in the third stage is determined mainly by the annihilation rate on the nitrogen buffer gas and on impurity molecules. Using a liquid nitrogen dewar inside the vacuum chamber to pump impurities, we have been able to reduce impurity effects so that the lifetime is typically about 45 s with the buffer gas present and increases to greater than 1700 s if the buffer gas feed is switched off after the loading phase. This is illustrated in Fig. 2(b), which also shows electron confine-

ment properties under the same conditions.

Typical parameters for the positron plasmas are as follows: maximum number of positrons trapped, $N=1.7\times10^7$, plasma radius, $\rho_p\sim2$ cm, plasma length, $L\sim5$ cm, positron number density, $n\sim2\times10^5$ cm^{-3}, Debye length, $\lambda_D\sim0.2$ cm, number of positrons in a Debye sphere, $N_D\sim10^4$.

III. PLASMA DIAGNOSTICS

A. Density and radial profile

Radial profiles of pure electron plasmas are commonly measured by dumping the plasma onto either movable collectors,[17] arrays of fixed collectors,[15] or concentric rings.[18] Recently, full two-dimensional imaging systems for pure electron plasmas have been developed. These systems involve the dumping of the plasmas onto microchannel plates[19] or phosphor screens.[20]

For our experiments, we assume the particle density $n(r,z)$ to be independent of the azimuthal coordinate and we employ concentric ring collectors. We dump the plasma onto the collector plates by dropping the potential on one of the confining electrodes, and we measure the charge striking each plate using a charge-sensitive amplifier. This yields a measurement of the z-integral of the density. A computer calculation is then used to deduce the density from this data, assuming the density along each magnetic field line (each r) follows the Boltzmann distribution for the measured temperature T and the self-consistently determined potential $\Phi(r,z)$.

B. Plasma temperature

The plasma temperature is measured using a "magnetic beach" temperature analyzer, which was originally developed as a neutral plasma diagnostic[21] and was later applied to pure electron plasmas.[22] A bias voltage V is applied to the collector plates and the curve $N(V)$ of the number of particles reaching the plates vs V is recorded. Then a magnetic mirror field is applied at the collectors and the curve is retaken. The curves are analyzed near their half-maximum points, and the perpendicular temperature in eV is found from the relation

$$k_bT=\frac{\partial N/\partial R}{\partial N/\partial V},$$

where R is the mirror ratio at the collector plates and is adjusted to be unity in the unmirrored case.

C. Diagnostics using plasma modes

For positron plasmas, the various techniques described above requiring dumping the plasma are not desirable, because the plasmas may take 60 s or longer to accumulate. Using electron plasmas similar to the positron plasmas in size and shape, but with about twice the density, we have developed a nondestructive method of monitoring plasma parameters using the properties of the global plasma modes studied by Dubin.[23,24]

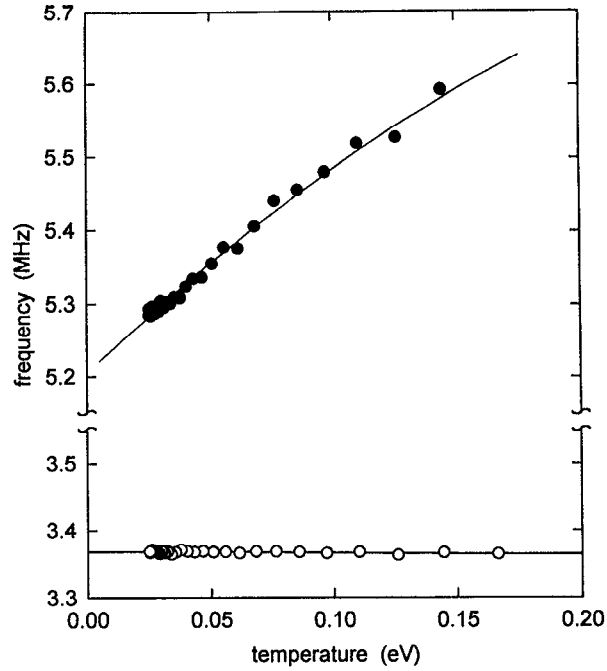

FIG. 3. Frequency of the quadrupole mode (●), and the center-of-mass mode (○), as a function of temperature for a typical electron plasma. The upper solid curve is from a numerical simulation. The lower solid line is a linear regression.

With the plasma confined in a hyperboloidal electrode structure [see Fig. 1(b)], the low-temperature equilibrium is a uniform-density spheroid. Dubin's cold fluid theory predicts the frequencies of all the normal modes of such a plasma, and these frequencies depend only on the plasma aspect ratio α, the ratio of plasma length to diameter. The theory has been verified by the Ion Storage Group at the National Institute of Standards and Technology for a few of the long-wavelength plasma modes of cryogenic pure ion plasmas.[25] That group also used the technique to deduce the aspect ratios of cryogenic pure electron plasmas.[26] At higher temperatures, the plasma pressure changes the equilibrium shape and contributes an added restoring force, with the net effect that the mode frequencies increase.

We have measured the temperature dependence of the quadrupole mode. The data in Fig. 3 for a typical electron plasma show that even at 300 K, the lowest temperature achieved in our experiments, the temperature effect is significant. In this figure we also show the frequency of the center-of-mass mode, which does not display any significant variation as the plasma is heated. This behavior is expected because the center-of-mass mode is not a collective plasma mode, but results from the bulk motion of the plasma. We can use measurements of the quadrupole mode frequency to observe changes in the plasma temperature or, at a known temperature, to observe changes in the plasma shape.[27] The latter approach is expected to be useful for long-term confinement studies.

The total particle number is found by measuring the amplitude of the plasma response at the fundamental harmonic frequency of the trap. In the quadratic potential

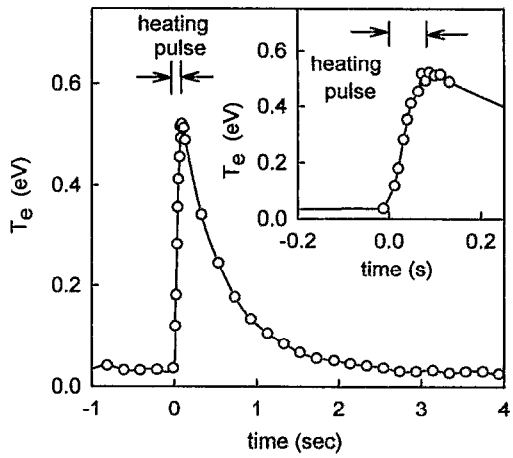

FIG. 4. (a) Electron temperature, measured using the magnetic beach analyzer, during a cycle of RF heating followed by a gas cooling phase. At $t=0$, a 100 ms burst of RF noise is applied. Inset: detail of the temperature during the noise burst.

created by this electrode structure, this frequency is a constant, and the number of particles is simply proportional to the amplitude of the response as long as the effects of image charges are not strong.

IV. MANIPULATION OF STORED PLASMAS

A. Heating and cooling

The trapping mechanism that we use involves reducing the energy of the incident positrons by means of inelastic collisions with the nitrogen buffer gas. The initial trapping collisions involve an electronic excitation collision which reduces the positron energy by about 8 to 9 eV. The positrons then cool to room temperature by means of rotational and vibrational excitation of the nitrogen molecules. For studying temperature dependences of plasma phenomena, it is useful to be able to manipulate the temperature after the plasma has been loaded. For long cylindrical electron plasmas, adiabatic compression or expansion of the plasma along the field has been used. The compressions can be applied either as a single pulse or by oscillating the confining potentials at a suitable frequency.[18,22]

We have recently developed a technique for heating the plasma by applying a radio frequency (RF) signal to one of the confining electrodes. In addition to studying the temperature dependence of electron plasma modes, it has also given us more insight into the cooling processes involved. In Fig. 4 we show the heating and cooling of electrons following the application of an RF heating pulse, which consists of broadband RF noise (10 kHz–10 MHz). Pulses of 0.1–1 ms duration and amplitude ~0.5 V are sufficient to produce significant heating, which appears to be stochastic in nature.

Using this heating technique, large temperature increases can be obtained in very short intervals. For example, if no buffer gas is present, the plasma can be heated from 0.025 eV to about 3 eV, i.e., by more than two orders of magnitude in less than 1 ms. If a nitrogen buffer gas is present, the temperature saturates at a lower level, typically about 0.3 to 0.5 eV, because the inelastic collision cross section for nitrogen increases rapidly above this energy.

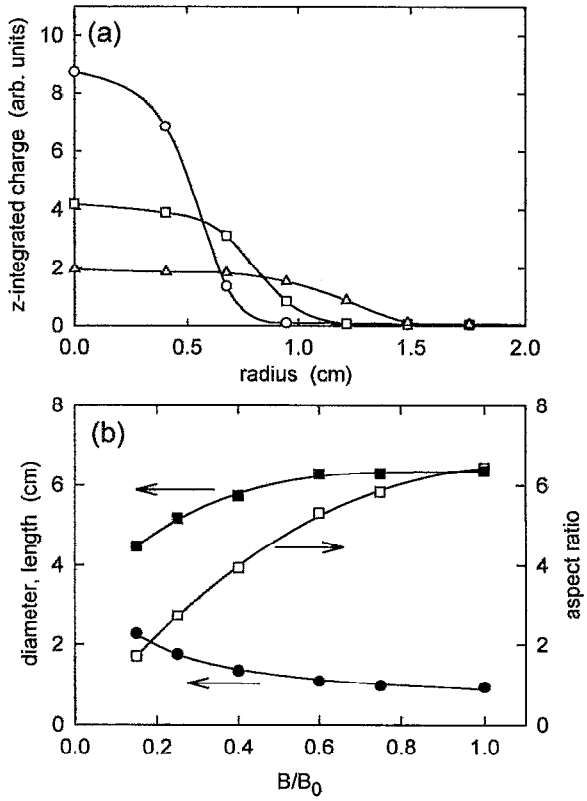

FIG. 5. (a) z-integrated radial profiles showing the expansion of the plasma by reduction of the magnetic field: 1460 G (○), 730 G (□), 365 G (△). (b) plasma diameter (●), plasma length (■), and aspect ratio (□), of an electron plasma as a function of the ratio of the final magnetic field B to the initial field B_0. The curve fitted to the plasma diameter D has the form $D \propto B^{-1/2}$. The curves fitted to the squares are polynomials.

B. Plasma expansion

For the study of plasma modes as remote diagnostics, it is desirable to be able to change the shape of the plasma in a controllable way. We have found that the most satisfactory method of accomplishing this is to reduce slowly the strength of the confining magnetic field B after the positrons or electrons have been loaded into the trap. This technique was first developed in cylindrical electron plasmas.[17]

Figure 5(a) shows typical radial profiles for the expansion of a plasma loaded with an initial magnetic field of $B=1460$ Gauss, while Fig. 5(b) shows how the plasma radius, length, and aspect ratio vary with B. The diameter of the plasma scales as $B^{-1/2}$ [shown by the curve fitted to the solid points in Fig. 5(b)], while line-integrated charge scales as B. The reduction in the line-integrated charge density has the effect of reducing the plasma length, as shown in Fig. 5(b). Both these effects act to reduce aspect ratio, which is also shown in this figure.

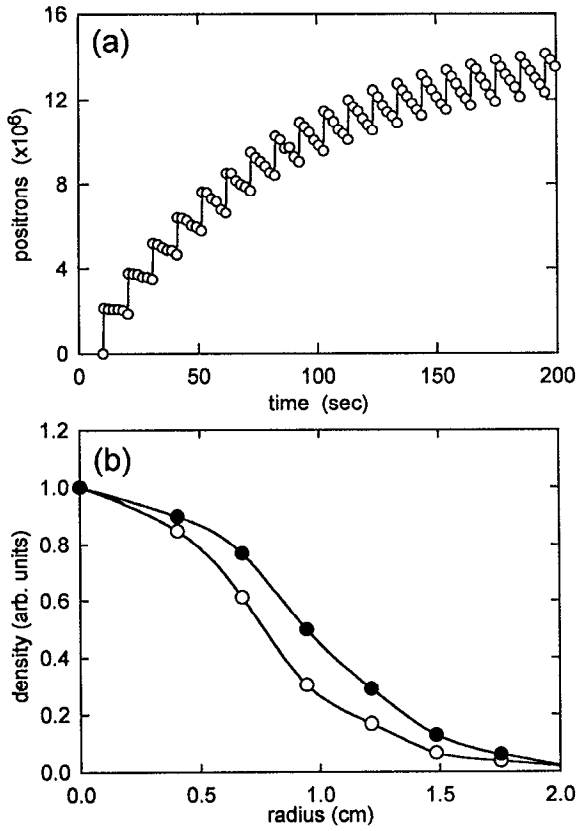

FIG. 6. (a) Number of positrons stored in the fourth stage through successive stackings. (b) z-integrated radial profiles for stacked plasmas after one stacking pulse (○), and after 20 stacking pulses (●).

C. Stacking

In order to increase the number of positrons available, we have recently implemented the technique known as stacking.[17] Positrons are loaded into the third stage for a period shorter than the lifetime in that stage, and then transferred to the fourth stage shown in Fig. 1, thereby building up a denser plasma. The transfer is accomplished by dropping the potential on the electrode between stage III and stage IV, as shown in the figure, and at the same time slightly raising the potential of stage III.

The gas pressure is slightly lower in the fourth stage and, furthermore, impurities are more effectively reduced by the proximity to the dewar and the fact that the electrodes are at a lower temperature. This increases the lifetime, by about a factor of 2. In Fig. 6(a) we show the positron count in the fourth stage during successive stacking pulses of 10 s duration. In Fig. 6(b), we show the plasma profiles after the first stacking pulse and after 20 pulses, each of 5 s duration. For easier comparison, the profiles have been normalized to their central value. These profiles show that the radius of the stacked plasma increases by only about 20% during the stacking sequence. Furthermore, this expansion can be explained by the viscous drag of the buffer gas, so the stacking process does not seem to expand the plasma unduly.

V. ELECTRON–POSITRON PLASMA PHYSICS ISSUES

A. Confinement studies

Although electron–positron (e^+e^-) plasmas have been discussed in a number of theoretical papers, they have not yet been created in the laboratory. Such plasmas are unique and will permit the study of the physics of equal-mass plasmas in ways that are not possible with negative-ion/positive-ion plasmas composed of particles of comparable mass, which have already been created in laboratory experiments. It is difficult to remove small amounts of residual electrons from these plasmas, and these electrons can efficiently screen the plasma response due to the ions. An important feature of e^+e^- plasmas is that both charge species are highly magnetized. The e^+e^- plasma system therefore permits the investigation of plasma confinement concepts by varying the plasma character continuously from the single species to the neutral plasma limit, in the case where both particles have the same high degree of magnetization. The creation of e^+e^- plasmas in the laboratory would also permit experimental studies of electron–positron vortex dynamics. Such experiments would be an extension of vortex studies that have been carried out in pure electron plasmas by Driscoll *et al.*[28]

B. Linear modes

Electron–positron plasmas have been considered theoretically by a number of authors. The simplest theoretical considerations involve description of the linear modes, which were discussed by Tsytovich and Wharton.[6] Recently, this subject was revisited in greater detail by Iwamoto.[7]

There are a number of results unique to this case of an equal-mass, opposite-charge plasma. In particular, some of the modes are distinctly different than those both in pure electron plasmas and in conventional neutral plasmas, where $m_e \ll m_i$. For the unmagnetized e^+e^- plasmas, the Bohm–Gross mode is undamped, but the ion acoustic mode is heavily damped in an equilibrium plasma having $T_{e^+} \sim T_{e^-}$. In magnetized e^+e^- plasmas, the dielectric constants for left and right circularly polarized waves propagating along the field are equal. There is an Alfvén wave, but no helicon or whistler waves. Cyclotron waves can have linear polarization.

For waves propagating perpendicular to the magnetic field, the dielectric tensor for the cold plasma is diagonal. Thus the extraordinary wave is purely transverse, and it is the same as the transverse wave that propagates along the magnetic field. For the warm plasma case, there are corrections due to cyclotron motion.

C. Nonlinear effects

There are many nonlinear effects that are different in e^+e^- plasmas than in more conventional plasmas. It is expected that "clump" and "hole" phenomena, first discussed by Dupree and co-workers are more pronounced for the equal mass case.[29] This can lead to a lowered threshold

for instabilities such as the current-driven ion acoustic instability, that would exist in e^+e^- plasmas with different positron and electron temperatures.

A number of nonlinear effects have been discussed by Tsytovich and Wharton.[6] One phenomenon is an exact cancellation of the coupling that leads to three-wave processes, so that Raman and Brillouin instabilities are absent. They also predict that, due to the heavy damping of ion acoustic waves, nonlinear effects, such as the occurrence of solitons, should be more prominent.

VI. ELECTRON–POSITRON PLASMA EXPERIMENTS

A. Paul trapping of electrons and positrons

The Paul trap[30] is the only technique of which we are aware that can confine both signs of charge with long confinement times. Schermann and Major used this technique to confine simultaneously both negative and positive ions (I^- and Tl^+) with confinement times of the order of a few seconds.[31] They found that a He buffer gas was necessary to achieve this good confinement. There are, however, potential problems in using a buffer gas in an RF trap with light particles such as electrons or positrons. Unlike the Penning trap where a buffer gas has a powerful cooling effect, in an RF trap elastic collisions act as a cooling process only if the buffer gas is much lighter than the particles being confined. This effect arises because elastic collisions with heavy particles at low energy result in large-angle scattering that dephase the orbits with respect to the RF field.

Inelastic collisions, on the other hand, will act as a cooling process in an RF trap. Therefore, a net cooling effect could possibly be obtained with a judicious choice of buffer gas. The ideal buffer gas would have as small an elastic collision cross section as possible and at the same time would have a large cross section for some inelastic process. For the energies of interest, i.e., ~ 1 eV, the most likely candidate process would be vibrational excitation. This is also an attractive process for the cooling mechanism because of the large fractional energy loss in each collision. Several substances have larger cross sections for vibrational excitation than elastic scattering in the region of energies 0.1–2 eV; specific examples include CF_4, SiH_4, Si_2H_6, and CCl_2F_2.

B. Electron-beam/positron-plasma experiments

Electron-beam/positron-plasma experiments are the simplest electron–positron experiments to perform because they do not require the simultaneous confinement of both species. We have constructed an electron gun and have commenced experiments of this type. The gun consists of an indirectly heated oxide-coated cathode with two grids for control of electron current and beam energy. The gun can supply controllable currents which enable us to explore the range of parameter space from $n_{e+} \ll n_{e-}$ to $n_{e+} \gg n_{e-}$.

Experiments will involve transmitting the electron beam through a confined plasma with an axial potential profile like that shown in Fig. 7. Diagnostics include: (1) measurement of modes excited in the plasma by observing signals on the confining electrodes. (2) Measurement of modulation of the electron beam intercepted by the collector plates. (3) Observing modifications to the positron plasmas by dumping following the beam transit.

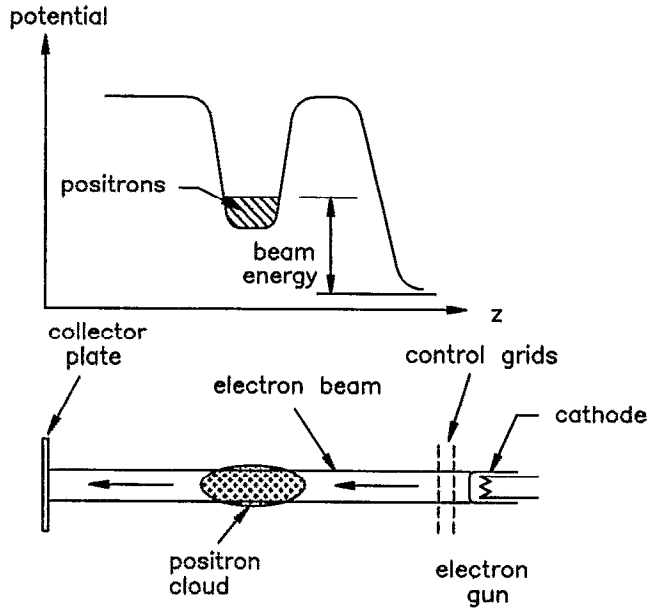

FIG. 7. Axial potential profile for the electron-beam/positron-plasma experiment shown.

VII. POSITRON MOLECULE INTERACTIONS

The clouds of room-temperature positrons that we can now accumulate are ideal for the study of positron annihilation in a controlled environment. This has opened up a new range of positron annihilation experiments that can be performed.

A. Positron annihilation experiments

Positron annihilation rates can be measured accurately using positron plasmas in traps because, at the low pressures attained, two-body collisions dominate. Positron annihilation rates on large molecules have been found to be anomalously high,[32,33] probably due to resonant binding of positrons to the molecule. We have measured annihilation rates for a number of substances and have identified chemical trends which may help in understanding the binding mechanism.[32–34] Our newly developed capability of controlling the positron temperature now enables us to measure temperature dependence of the annihilation rates.

When a positron annihilates on a molecule, the gamma-ray annihilation line is Doppler broadened as a result of the momentum of the annihilated electron. This broadening can be measured by high-resolution gamma-ray detectors. An example of the type of spectra that can be obtained is given in Fig. 8. We recently undertook a comprehensive study of annihilation linewidths, including a range of hydrocarbons and perfluorocarbons.[10] Studies of this type are of importance in interpreting gamma-ray

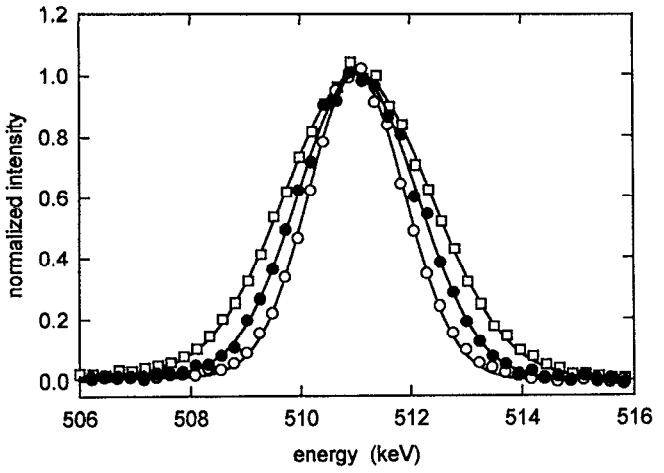

FIG. 8. Typical gamma-ray spectra from *in situ* annihilation of positrons on hydrogen (○), hexane (●), and carbon tetrachloride (□). The solid curves are fitted Gaussians. The data have been normalized to the maxima of the fitted curves. When corrected for the instrumental resolution of 1.15 keV, these data yield energy widths (full width, half maximum) of 1.72 ± 0.03 keV, 2.29 ± 0.03 keV, and 2.9 ± 0.03 keV for hydrogen, hexane, and carbon tetrachloride, respectively.

spectra of astrophysical origin,[35,34] and may also give insight into positron binding on large molecules by providing information on the localization of the positron on the molecule.

Another technique that has emerged from our positron annihilation experiments is positron ionization mass spectrometry (PIMS).[36–38] The annihilation of a positron with an electron on a molecule can produce both fragmented and unfragmented ions. The masses of these ions may be determined by time-of-flight spectrometry or by ion cyclotron resonance mass spectrometry.

B. Astrophysical simulations

Studies of the energy distribution of astrophysical, positron-annihilation gamma rays show a narrow peak superimposed on a broader distribution. This is believed to result from the slowing down of energetic positrons by collisions with the interstellar medium. The broad peak is produced by positrons that form positronium atoms at moderate energies, whereas positrons which drop below the positronium formation energy threshold before annihilating generate the narrow peak. The widths of the two components and their relative strengths provide information on the composition of the interstellar medium.

It has been predicted[39] that in clouds of atomic hydrogen, the annihilation linewidth and the fraction of annihilations occurring through positronium formation are strong functions of the degree of ionization of the gas. Positrons can neither annihilate with protons nor lose significant energy during collisions with them, so the positronium fraction is determined by the competition between energy loss by collisions with electrons and positronium formation by collisions with gas atoms. For sufficiently high ionization fraction, the energy loss will be fast enough that few positrons will form positronium in flight before the process becomes energetically impossible. The critical ionization fraction separating qualitatively different regimes is believed to be in the range $0.01 \leqslant \eta_c \leqslant 0.1$.

This prediction has never been tested experimentally. Since the protons are nearly irrelevant to positron slowing down, a partially ionized atomic hydrogen gas could be simulated using an electron plasma and neutral molecular hydrogen. A positron beam could be passed through the gas–plasma system, and the gamma-ray spectrum of the resulting annihilations recorded for various beam energies. The virtue of this design is that the "ionization fraction" (i.e., the ratio of electron density to electron plus neutral H_2 density) can be varied by simply changing the H_2 pressure at a fixed electron density.

VIII. FUTURE IMPROVEMENTS

It would be desirable to increase the number of positrons available for experiments. In the present configuration, there are two limitations on the number of trapped positrons, namely, the positron filling rate and the positron lifetime in the final stage of the trap.

The positron lifetime is determined by annihilation on the gas and transport out of the trap. As described in Sec. II, annihilation has been found to be the dominant loss mechanism. The recently installed demonstration fourth stage has a lifetime about twice that of the present third stage and can be loaded by stacking the positrons from the third stage. We plan to construct a separate ultrahigh vacuum fourth stage with higher magnetic field to provide cooling by cyclotron radiation. This will enable us to increase the lifetime by at least two orders of magnitude over the present value and will enable us to accumulate positrons over extended periods. These large clouds of positrons can be used for experiments directly or can be used as a reservoir for pulsed experiments by repetitively extracting bunches of positrons.

The filling rate is limited mainly by the low efficiency of the tungsten transmission moderator. An attractive alternative to this type of moderator is the solid rare gas moderator developed by Mills and Gullikson.[40] They obtain an efficiency of 0.3% from a 100 mCi ^{22}Na source using a solid neon moderator. Recently, they have obtained almost as good an efficiency from solid krypton.[41] Using such a moderator, we could increase our positron filling rate by a factor of about 10, i.e., to about 4 million positrons per second.

IX. CONCLUSION

The positron plasmas made possible by recent advances in trapping techniques have sufficient size and density to be useful in experiments ranging from electron–positron plasmas to positron–molecule interactions. Improvements in plasma handling and temperature control and measurement have led to the development of techniques for the remote monitoring of plasma size and temperature. An electron-beam/positron-plasma experiment now underway is the first experimental study of electron–

positron plasma physics, a potentially rich subject of importance to basic plasma physics and astrophysics. The new experimental capabilities also will allow extension of positron–molecule experiments to higher energies. These studies have found anomalously high annihilation cross sections for many molecules at low energies, with interesting implications for gamma-ray astrophysics as well as molecular physics. Anticipated improvements in the moderator and in the lifetime of the trapped positrons are expected to be particularly important for the experiments with electron–positron plasmas.

ACKNOWLEDGMENTS

We wish to acknowledge useful discussions with D. H. E. Dubin, K. Iwata, M. Leventhal, G. W. Mason, T. J. Murphy, T. M. O'Neil, and R. L. Spencer, and the expert technical assistance of E. A. Jerzewski.

This work is supported by the Office of Naval Research and the National Science Foundation under Grant No. PHY 9221283.

[1]T. J. Murphy and C. M. Surko, Phys. Rev. A **46**, 5696 (1992).
[2]W. Wolfer, Ph.D. thesis, University of Florida, 1969.
[3]R. J. Gould, Physica **60**, 145 (1972).
[4]R. J. Gould, Astrophys. J. **344**, 232 (1989).
[5]H. Alfvén, *Cosmic Plasma* (Reidel, Boston, 1981).
[6]V. Tsytovich and C. B. Wharton, Comments Plasma Phys. Controlled Fusion **4**, 91 (1978).
[7]N. Iwamoto, Phys. Rev. E **47**, 604 (1993).
[8]C. M. Surko, M. Leventhal, and A. Passner, Phys. Rev. Lett. **62**, 901 (1989).
[9]G. Gabrielse, X. Fei, L. A. Orozco, R. L. Tjoelker, J. Haas, H. Kalinowsky, T. A. Trainor, and W. Kells, Phys. Rev. Lett. **63**, 1360 (1989).
[10]S. Tang, M. D. Tinkle, R. G. Greaves, and C. M. Surko, Phys. Rev. Lett. **68**, 3793 (1992).
[11]C. M. Surko, R. G. Greaves, and M. Leventhal, Hyperfine Interactions **81**, 239 (1993).
[12]G. Gabrielse, S. L. Rolston, L. Haarsma, and W. Kells, Phys. Lett. A **129**, 38 (1988).
[13]E. Gramsch, J. Throwe, and K. G. Lynn, Appl. Phys. Lett. **51**, 1862 (1987).
[14]K. G. Lynn, B. Nielsen, and J. H. Quateman, Appl. Phys. Lett. **47**, 239 (1985).
[15]J. H. Malmberg and C. F. Driscoll, Phys. Rev. Lett. **44**, 654 (1980).
[16]C. F. Driscoll, J. H. Malmberg, and K. S. Fine, Phys. Rev. Lett. **60**, 1290 (1988).
[17]J. H. Malmberg, C. F. Driscoll, B. Beck, D. L. Eggleston, J. Fajans, K. Fine, X.-P. Huang, and A. W. Hyatt, in *Non-neutral Plasma Physics*, edited by C. W. Roberson and C. F. Driscoll (American Institute of Physics, New York, 1988), pp. 28–71.
[18]B. R. Beck, J. Fajans, and J. H. Malmberg, Phys. Rev. Lett. **68**, 317 (1992).
[19]A. J. Peurrung and J. Fajans, Rev. Sci. Instrum. **64**, 52 (1993).
[20]K. S. Fine, C. F. Driscoll, and X. P. Huang, Bull. Am. Phys. Soc. **38**, 1971 (1993).
[21]D. Boyd, W. Carr, R. Jones, and M. Seidl, Phys. Lett. A **45**, 421 (1973).
[22]A. W. Hyatt, C. F. Driscoll, and J. H. Malmberg, Phys. Rev. Lett. **59**, 2975 (1987).
[23]D. H. E. Dubin, Phys. Rev. Lett. **66**, 2076 (1991).
[24]D. H. E. Dubin, Phys. Fluids B **5**, 295 (1993).
[25]J. J. Bollinger, D. J. Heinzen, F. L. Moore, W. M. Itano, D. J. Wineland, and D. H. E. Dubin, Phys. Rev. A **48**, 525 (1993).
[26]C. S. Weimer, J. J. Bollinger, F. L. Moore, and D. J. Wineland, "Electrostatic modes as a diagnostic in penning trap experiments," submitted to Phys. Rev. A (1993).
[27]M. D. Tinkle, R. G. Greaves, C. M. Surko, R. L. Spencer, and G. W. Mason, Phys. Rev. Lett. **72**, 352 (1994).
[28]C. F. Driscoll and K. S. Fine, Phys. Fluids B **2**, 1359 (1990).
[29]R. H. Berman, D. J. Tetreault, and T. H. Dupree, Phys. Fluids **28**, 155 (1985).
[30]W. Paul, Rev. Mod. Phys. **62**, 531 (1990).
[31]J. P. Schermann and F. G. Major, Appl. Phys. **16**, 225 (1978).
[32]T. J. Murphy and C. M. Surko, Phys. Rev. Lett. **67**, 2954 (1991).
[33]C. M. Surko, A. Passner, M. Leventhal, and F. J. Wysocki, Phys. Rev. Lett. **61**, 1831 (1988).
[34]K. Iwata, R. G. Greaves, and C. M. Surko, "Annihilation rates of positrons on aromatic molecules," to be published in Hyperfine Interactions.
[35]M. Leventhal, S. D. Barthelmy, N. Gehrels, B. J. Teegarden, J. Tueller, and L. M. Bartlett, Astrophys. J. Lett. **405**, L25 (1993).
[36]A. Passner, C. M. Surko, M. Leventhal, and A. P. Mills, Jr., Phys. Rev. A **39**, 3706 (1989).
[37]J. Xu, L. D. Hulett, Jr., T. A. Lewis, D. L. Donohue, S. A. McLuckey, and G. L. Glish, Phys. Rev. A **47**, 1023 (1993).
[38]G. L. Glish, R. G. Greaves, S. A. McLuckey, L. D. Hulett, C. M. Surko, J. Xu, and D. L. Donohue, "Ion production by positron-molecule resonances," to be published in Phys. Rev. A.
[39]R. W. Bussard, R. Ramaty, and R. J. Drachman, Astrophys. J. **228**, 928 (1979).
[40]A. P. Mills, Jr. and E. M. Gullikson, Appl. Phys. Lett. **49**, 1121 (1986).
[41]T. Grund, K. Maier, and A. Seeger, Materials Science Forum **105–110**, 1879 (1992).